

Temperature-dependent Presteady State Kinetics of Lumazine Synthase from the Hyperthermophilic Eubacterium *Aquifex aeolicus**

Received for publication, March 26, 2003, and in revised form, June 12, 2003
Published, JBC Papers in Press, July 16, 2003, DOI 10.1074/jbc.M303090200

Ilka Haase, Markus Fischer, Adelbert Bacher, and Nicholas Schramek‡

From the Lehrstuhl für Organische Chemie und Biochemie, Technische Universität München, Lichtenbergstr. 4, D-85747 Garching, Germany

6,7-Dimethyl-8-ribityllumazine synthase (lumazine synthase) catalyzes the condensation of 5-amino-6-ribitylamino-2,4(1*H*,3*H*)-pyrimidinedione and 3,4-dihydroxy-2-butanone 4-phosphate. Presteady state kinetic experiments using the enzyme from the hyperthermophilic bacterium *Aquifex aeolicus* were monitored by multiwavelength photometry. An early optical transient absorbing around 330 nm is interpreted as a Schiff base intermediate obtained by reaction of the position 5 amino group of the heterocyclic substrate with the carbonyl group of 3,4-dihydroxy-2-butanone 4-phosphate. A second transient with an absorption maximum at 445 nm represents an intermediate resulting from the elimination of orthophosphate from the Schiff base. The rate-determining step is the subsequent formation of the 7-exomethylene type anion of 6,7-dimethyl-8-ribityllumazine. The rate constants for the three partial reactions identified by the stopped flow experiments show linear Arrhenius relations in the temperature range of 15–70 °C.

6,7-Dimethyl-8-ribityllumazine synthase catalyzes the condensation of 5-amino-6-ribitylamino-2,4(1*H*,3*H*)-pyrimidinedione (**2**) with 3,4-dihydroxy-2-butanone 4-phosphate (**1**), affording inorganic phosphate, water, and the riboflavin precursor, 6,7-dimethyl-8-ribityllumazine (**3**) (Fig. 1) (1–4). The enzyme from the hyperthermophilic eubacterium, *Aquifex aeolicus*, is an essentially spherical capsid of 60 identical subunits with icosahedral 532 symmetry (5). Structurally similar enzymes have been observed in *Bacillus subtilis*, *Escherichia coli*, and spinach (6–9). The *B. subtilis* enzyme can form a complex with a homotrimeric riboflavin synthase molecule enclosed in the core of the icosahedral capsid (10–13). That enzyme complex catalyzes the synthesis of 1 eq of riboflavin (**4**) and 2 eq of inorganic phosphate from 1 eq of 5-amino-6-ribitylamino-2,4(1*H*,3*H*)-pyrimidinedione (**2**) and 2 eq of 3,4-dihydroxy-2-butanone 4-phosphate (**1**) (11, 14). It is unknown whether lumazine synthase of *A. aeolicus* can form a similar heterooligomeric complex.

A hypothetical reaction mechanism for lumazine synthase is shown in Fig. 2 (2). Briefly, the 5-amino group of the pyrimidine derivative **2** is believed to react with the carbonyl group of

compound **1**, and the resulting Schiff base **5** then eliminates orthophosphate. Keto-enol tautomerization of the resulting intermediate **7** is followed by ring closure via intramolecular condensation, affording **9**. The final reaction step could be the elimination of water from the covalent hydrate **9** followed by protonation of the resulting lumazine anion **10** (compare Fig. 3).

On the basis of x-ray crystallographic studies (15, 16), the Schiff base intermediate **5** is believed to be bound in an extended conformation. Thus, a rotation of the position 5 side chain of one of the proposed intermediates **5** or **6** must precede the formation of the pyrazine ring.

Presteady state kinetics of lumazine synthase of *B. subtilis* have been studied in some detail (17). The most salient feature of those studies was a transient species with an absorbance maximum at 455 nm. In an earlier stopped flow study with lumazine synthase of *E. coli* (18), the absorption of that reaction intermediate had been assigned to the final reaction product **3** as a consequence of insufficient instrumentation.

Lumazine synthase from the hyperthermophilic eubacterium *A. aeolicus* is stable and catalytically active at temperatures up to at least 90 °C (5, 15). The thermal stability of the protein in conjunction with the favorable spectroscopic properties of certain reaction intermediates prompted a presteady state kinetic analysis over a wide range of temperatures.

EXPERIMENTAL PROCEDURES

Materials—3,4-Dihydroxy-2-butanone 4-phosphate was prepared from ribose 5-phosphate using recombinant 3,4-dihydroxy-2-butanone 4-phosphate synthase (19). 5-Nitro-6-ribitylamino-2,4(1*H*,3*H*)-pyrimidinedione (**20**) and 6,7-dimethyl-8-ribityllumazine (**21**) were synthesized by published procedures. 5-Amino-6-ribitylamino-2,4(1*H*,3*H*)-pyrimidinedione was freshly prepared as described (11).

Enzyme Purification—Recombinant lumazine synthase of *A. aeolicus* was purified by published procedures (5).

Enzyme Assay—Catalytic activity of lumazine synthase was determined as described elsewhere (22).

Equilibrium Dialysis—Equilibrium dialysis experiments were performed as published elsewhere (23).

Single Turnover Experiments—Stopped flow experiments were performed using an SFM4/QS apparatus from Bio-Logic (Claix, France) equipped with a linear array of three mixers and four independent syringes. The content of a 1.5-mm light path quartz cuvette behind the last mixer was monitored with a Tidas diode array spectrophotometer (200–610 nm) equipped with a 15-watt deuterium lamp as light source (J&M Analytische Mess- und Regeltechnik, Aalen, Germany). The enzyme solution was mixed with substrate solution at different temperatures at a ratio of 1:1 with a total flow rate of 4 ml s⁻¹. At that flow rate, the calculated dead time is 7.6 ms. Optical spectra integrated over 100 ms were recorded at intervals of 100 ms in the wavelength range of 240–500 nm.

Global Analysis of Stopped Flow Data—Prior to numerical analysis, the data were corrected for absorbance of buffer and enzyme by subtraction of a blank data set obtained without addition of sub-

* This work was supported by the Deutsche Forschungsgemeinschaft, the Fonds der Chemischen Industrie, and the Hans-Fischer-Gesellschaft. The costs of publication of this article were defrayed in part by the payment of page charges. This article must therefore be hereby marked "advertisement" in accordance with 18 U.S.C. Section 1734 solely to indicate this fact.

‡ To whom correspondence should be addressed. Tel.: 49-89-289-13361; Fax: 49-89-289-13363; E-mail: nicholas.schramek@ch.tum.de.

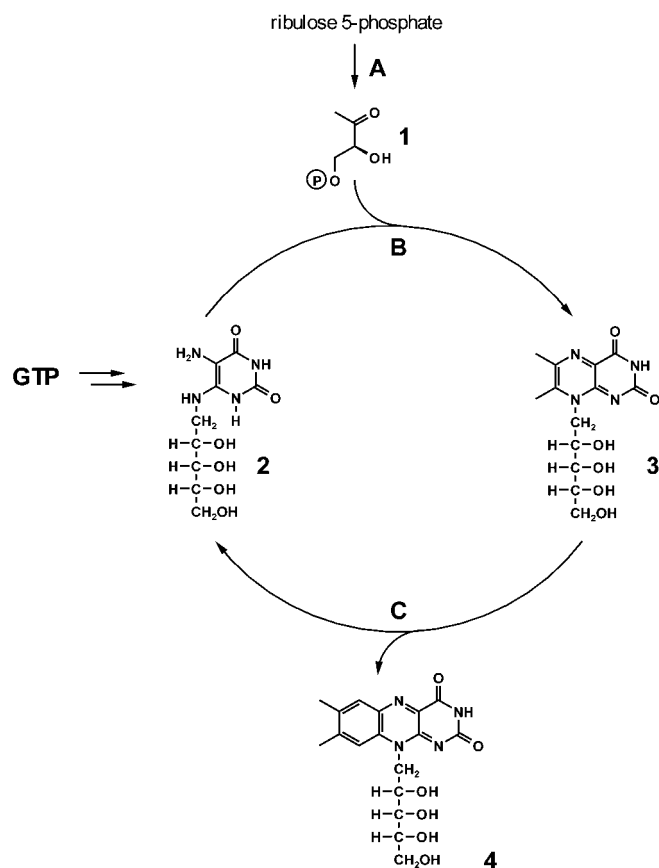


FIG. 1. **Biosynthesis of riboflavin.** A, 3,4-dihydroxy-2-butanone 4-phosphate synthase; B, 6,7-dimethyl-8-ribityllumazine synthase; C, riboflavin synthase.

strate. Data reduction and stronger weighting of early spectra were achieved by extracting 300 spectra on a pseudo-logarithmic time base from the difference data sets. These data sets were then analyzed using the program SPECFIT/32 3.0.32 (Spectrum Software Associates, Marlborough, MA).

RESULTS

Under steady state conditions at 37 °C, lumazine synthase of *A. aeolicus* was found to obey Lineweaver-Burke kinetics over a wide concentration range (data not shown). The catalytic rate at 37 °C is 31 nmol mg⁻¹ min⁻¹, and the K_m values for 5-amino-6-ribitylamino-2,4(1H,3H)-pyrimidinedione (2) and 3,4-dihydroxy-2-butanone 4-phosphate (1) are 10 and 26 μ M, respectively. The enzyme is catalytically active up to temperatures of at least 90 °C and obeys a linear Arrhenius relationship with remarkable accuracy (24). Activation parameters from steady state kinetic data analysis are summarized in Table I.

The enzyme product, 6,7-dimethyl-8-ribityllumazine (3), binds relatively tightly to *A. aeolicus* lumazine synthase ($K_D = 70 \mu$ M at pH 7.0 and 4 °C) as shown by equilibrium dialysis (data not shown). Binding is accompanied by a major change of the optical spectrum of the bound ligand. Although 3 in aqueous solution at neutral pH shows absorption maxima at 408 and 256 nm with a shoulder at 276 nm, the difference spectrum of 3 bound to lumazine synthase of *A. aeolicus* shows absorption maxima at 379 and 317 nm with a shoulder at 307 nm (Fig. 4A).

Rapid mixing of *A. aeolicus* lumazine synthase with the pyrimidine substrate 2 at 15 °C afforded the series of optical spectra shown in Fig. 5, which are characterized by a rapid decrease of absorption at 284 nm and a shift of the absorption maximum from 284 to 278 nm (spectra are corrected for protein absorption). Deconvolution using the program package

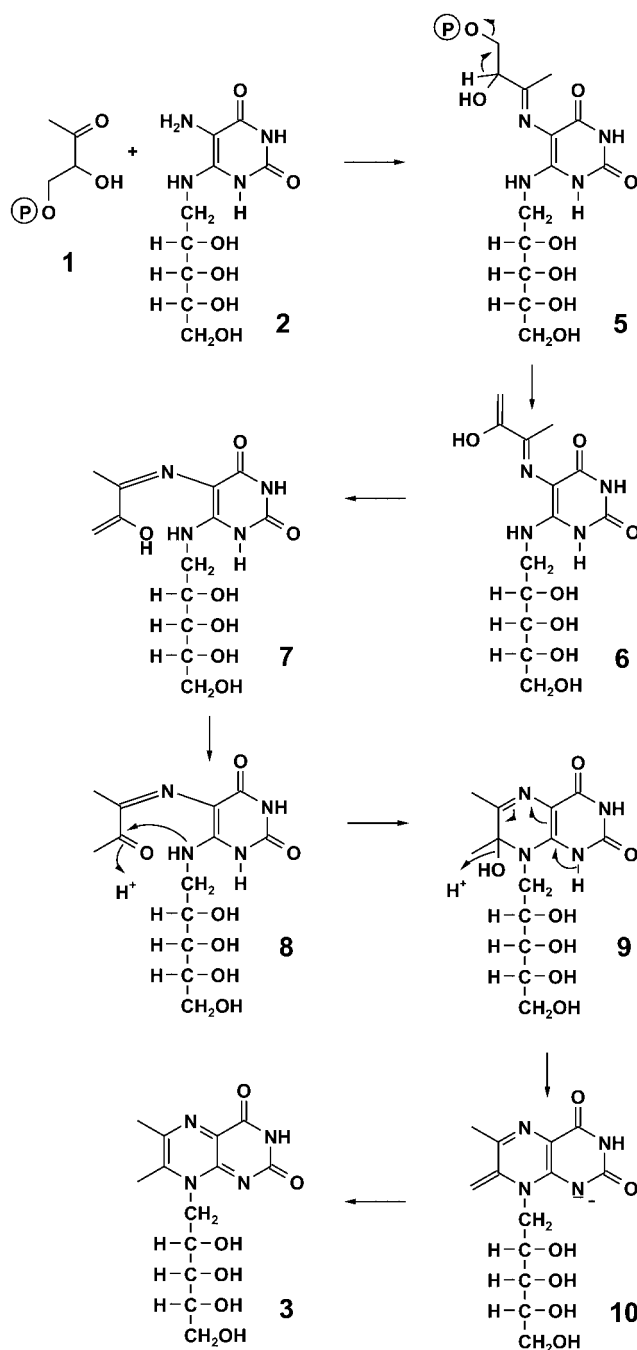


FIG. 2. **Hypothetical reaction mechanism of lumazine synthase (2).**

SPECFIT/32 revealed a single exponential process with a second order rate constant of 10.4 nM⁻¹ s⁻¹ at 15 °C. In line with the kinetic data, difference spectra recorded under steady state conditions confirmed that the absorbance of compound 2 is reduced by about 25% upon binding to the enzyme. Similar observations have been reported earlier in experiments with lumazine synthase of *B. subtilis* (17).

Fig. 6 shows a series of spectra obtained after rapid mixing of compound 2 with a solution containing compound 1 and protein at 25 °C. The concentrations after mixing were 96 μ M compound 2, 500 μ M compound 1, and 105 μ M enzyme subunits at pH 6.9. Since the carbohydrate type substrate 1 has no significant absorption in the spectral range used for analysis, it could be used in a relatively large excess to saturate the respective binding sites.

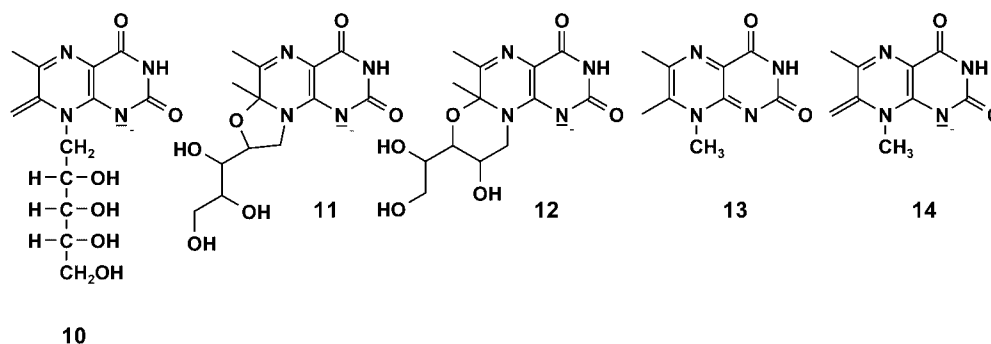


FIG. 3. Anionic species of 6,7-dimethyl-8-ribyllumazine (3) and 6,7,8-trimethylllumazine (13) (25–27).

TABLE I

Rate constants of partial reactions and activation parameters of lumazine synthase from *A. aeolicus* (data from presteady state experiments).

Reaction		Rate constants (25 °C)	E^a	ΔG^\ddagger	ΔH^\ddagger	$-T\Delta S^\ddagger$
			kJ mol^{-1}	kJ mol^{-1}	kJ mol^{-1}	kJ mol^{-1}
A \rightarrow B	k_1	$0.0334 \pm 0.0045 (\mu\text{M}^{-1} \text{s}^{-1})$	57.6 ± 6.7	81.4 ± 7.4	55.1 ± 6.7	26.3 ± 0.7
B \rightarrow C	k_2	$0.364 \pm 0.086 (\text{s}^{-1})$	75.3 ± 5.1	75.5 ± 10.1	72.8 ± 5.1	2.7 ± 5.0
C \rightarrow D	k_3	$0.0172 \pm 0.0016 (\text{s}^{-1})$	81.0 ± 1.0	83.1 ± 3.0	78.4 ± 1.5	4.7 ± 0.9
D \rightarrow E	k_4	$0.0034 \pm 0.0001 (\text{s}^{-1})$	76.1 ± 0.7	87.1 ± 1.4	73.5 ± 0.7	13.6 ± 0.7
A \rightarrow E ^a	k	$0.0027 \pm 0.0002 (\text{s}^{-1})$	74.3 ± 1.1	88.0 ± 2.3	72.0 ± 1.1	16.0 ± 1.0

^a Steady state kinetic experiment.

Selected spectra from Fig. 6 are shown in Fig. 7. The spectrum recorded 5 s after mixing shows a shoulder at about 330 nm. The subsequent reaction phase is characterized by transient absorption in the long wavelength range; the absorption at 445 nm passes through a maximum at 147 s (Fig. 8).

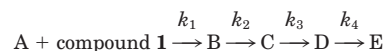
The final reaction phase shows highly characteristic spectra with maxima at 392, 318, and 247 nm. The spectrum recorded at 1100 s (Fig. 7B) is virtually identical with the difference spectrum of compound **3** bound to lumazine synthase under steady state conditions (compare Fig. 4A) but differs substantially from that of **3** in the absence of enzyme. It is therefore obvious that the enzyme product is predominantly present in the protein-bound form at the end of the reaction trajectory at the solute concentrations used in our experiments. For a more detailed analysis, the data set in Fig. 6 was subjected to singular value decomposition using the program SPECFIT/32 (Spectrum Software Associates), which indicated five linearly independent optical spectra significantly above the noise floor (Fig. 9A, spectra A–E).

The reconstructed transient spectrum A in Fig. 9A closely resembles that of free 5-amino-6-ribylamino-2,4-(1*H*,3*H*)-pyrimidinedione. The transient spectrum B (Fig. 9A) resembles the difference spectrum of that compound in complex with the enzyme (compare Fig. 5). Spectrum C has a maximum at 287 nm and a broad shoulder around 335 nm and is well in line with the expectations for a Schiff base derivative of **5**. Transient spectrum D is characterized by absorption maxima at 445 and 281 nm. The reconstructed spectrum E shows maxima at 391, 318, and 248 nm with shoulders at 310 and 285 nm and is similar to the difference spectrum of 6,7-dimethyl-8-ribyllumazine in complex with the enzyme (compare Fig. 4A). Reconstructed spectra similar to transients A–D have been reported in presteady state work with lumazine synthase of *B. subtilis*, whereas spectrum E differs from the final spectrum observed with the *B. subtilis* enzyme ((17); also, for details, see “Discussion” in this article).

Linear deconvolution of the data in Fig. 6 shows a rapid decrease of transient A (Fig. 9B). The half-life of that species is about 0.3 s at 25 °C. The transients B–D pass through maxima at 0.9, 12, and 142 s, respectively. Transient E begins to in-

crease monotonously after about 2 s, but more than 10 min are required at 25 °C for that transient to reach a plateau.

The data were numerically fitted to a kinetic model implicating four consecutive reaction steps according to Reaction 1,



REACTION 1

Using Reaction 1, the kinetic data in Fig. 6 can be modeled by a set of one second order reaction and three first order reactions. The numerical values of the rate constants k_1 to k_4 at pH 6.9 and at 25 °C are shown in Table I. The rate-limiting step is the transformation of the transient species D into E with a rate constant k_4 , which has a value of 0.003 s^{-1} at 25 °C. The lines in Fig. 9B were calculated using the parameters in Table I. The observed and simulated absorption values show excellent agreement (Fig. 8).

Since lumazine synthase of *A. aeolicus* is stable and catalytically active over a wide range of temperatures, stopped flow experiments could be performed at temperatures ranging from 15 to 70 °C. Throughout that temperature range, numerical deconvolution afforded transient spectra that were closely similar to those shown in Fig. 6. Fig. 10A shows time-dependent optical absorbance at 460 nm in stopped flow experiments in the temperature range of 15–70 °C. As described above (compare Fig. 9A), the intermediate species D absorbs at a longer wavelength than any other reaction component and can therefore be monitored easily without contribution by any other reactant species. This facilitates experiments over a wide range of temperatures. At each temperature studied, the absorption at 460 nm passes through a maximum and subsequently declines to very low values. The maximum amplitude is virtually the same at temperatures between 35 and 70 °C but becomes progressively lower at temperatures below 35 °C. The maximum amplitude is reached 392 s after mixing at 15 °C and 2.2 s after mixing at 70 °C. As shown in Fig. 10B, the logarithm of the time required to reach the maximum concentration of intermediate D is proportional to the temperature. The result is well in line with the hypothesis that the reaction profile is not

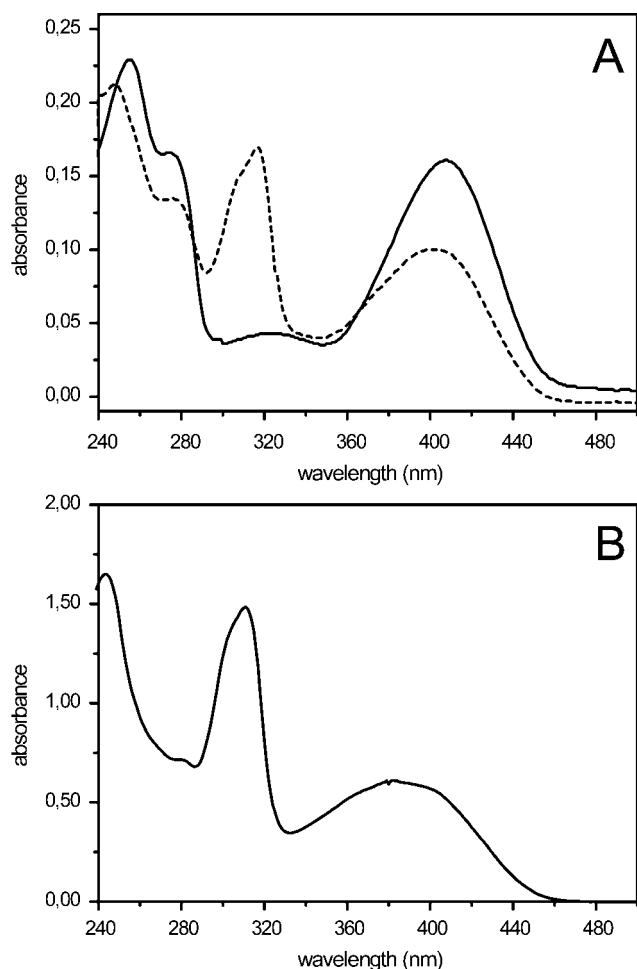


FIG. 4. A, absorption spectra of 6,7-dimethyl-8-ribityllumazine (**3**) at pH 6.9. *Solid line*, in aqueous solution; *broken line*, in complex with lumazine synthase of *A. aeolicus* (difference spectrum corrected for protein absorption at the same pH). B, absorption spectrum of 90 μM 6,7,8-trimethylumazine (**13**) in 100 mM potassium phosphate, pH 10.

significantly affected by the temperature dependence of the Michaelis-Menten constants.

The linear deconvolution of stopped flow experiments performed at different temperatures afforded values for k_1 to k_4 in the temperature range of 15–70 °C. The Arrhenius plots for k_1 to k_4 are all linear and have similar slopes (Fig. 11, Tables I and II). The resulting activation energies show values from 57 to 81 kJ mol^{-1} .

The free energy difference between free and bound compound **2** and between free and bound 6,7-dimethyl-8-ribityllumazine was calculated using the apparent dissociation constants of 4 and 70 μM , respectively ($\Delta G^\ddagger = -RT \ln K^\ddagger$). Thermodynamic activation parameters were calculated from the corresponding Eyring plots using the relationships $\ln(kT^{-1}) = -\Delta H^\ddagger R^{-1} T^{-1} + \ln(k_b h^{-1}) + \Delta S^\ddagger R^{-1}$ and $\Delta G^\ddagger = \Delta H^\ddagger - T\Delta S^\ddagger$, where k_b is Boltzmann's constant, h is Plack's constant, R is the gas constant, and ΔG^\ddagger , ΔH^\ddagger , and ΔS^\ddagger are the free energy, enthalpy, and entropy of activation, respectively. As shown in Tables I and II, data for ΔG^\ddagger , ΔH^\ddagger , and $-T\Delta S^\ddagger$ lie in the range of 75–88 kJ mol^{-1} , 55–79 kJ mol^{-1} , and 2–27 kJ mol^{-1} , respectively.

DISCUSSION

Due to a rare combination of properties, lumazine synthase of *A. aeolicus* is a particularly favorable experimental system for the presteady state kinetic analysis of a complex catalytic reaction sequence. (i) One of the substrates (compound **2**), two

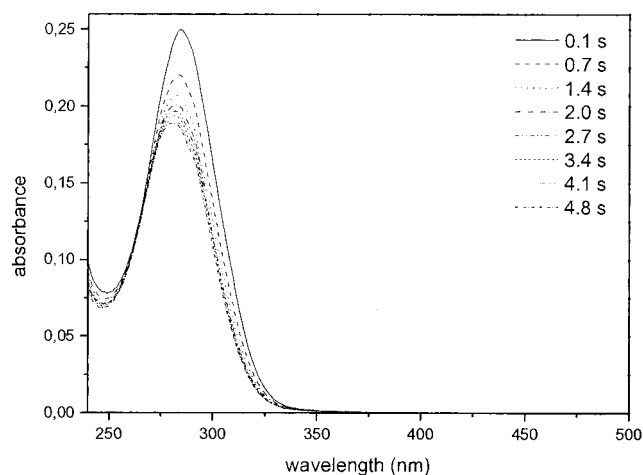


FIG. 5. **Binding of compound 2 to lumazine synthase.** Solutions of compound **2** and of lumazine synthase in 100 mM potassium phosphate, pH 6.9, were rapidly mixed at 15 °C. The concentrations after mixing were 96 μM compound **2** and 105 μM lumazine synthase subunits.

intermediates, and the product (compound **3**) have highly distinctive absorbance spectra that, together, cover a wide spectral range extending from ultraviolet into the visible range up to about 500 nm. Notably, the intermediates B and C absorb at longer wavelengths than their respective precursors. (ii) One of the substrates, the carbohydrate **1**, has no significant absorbance in the entire spectral range and can be used in stoichiometric excess to facilitate the kinetic analysis. (iii) The enzyme reaction is naturally slow by comparison with the dead time of stopped flow equipment. (iv) The enzyme of *A. aeolicus* can be prepared in large amounts and is stable and catalytically active over a wide range of temperatures.

The time-resolved ultraviolet spectra obtained with the enzyme from the hyperthermophilic *A. aeolicus* share many similarities with those obtained in our earlier study with the enzyme from the mesophilic *B. subtilis* but also display some surprising differences (17). With the enzymes from both microorganisms, the most rapid process is a decline of the pyrimidine absorption in conjunction with a slight wavelength shift. Since the second substrate, **1**, is not required for those absorption changes to take place, this rapid process is attributed to the formation of an enzyme-substrate complex. In line with that interpretation, the kinetics are well in line with a second order reaction (notably, the concentrations of the substrate **2** and of the protein subunits were closely similar in our experiments).

Extensive x-ray structure analysis of lumazine synthase in complex with a variety of ligands has shown that the pyrimidine substrate is bound at the active site of the *A. aeolicus* enzyme in close proximity to a phenylalanine residue, which forms a coplanar complex with the pyrimidine ring of the substrate (5, 16). The interaction between the π electron systems of the phenyl and pyrimidine residues of the protein and substrate, respectively, may be the reason for the relatively drastic modulation of the absorbance intensity of the bound ligand. However, we cannot rule out the possibility of a concomitant protonation or deprotonation process due to modulation of the pK of the substrate by the protein environment.

The temperature dependence of the rate constant k_1 describing the association of the protein and the pyrimidine type substrate is virtually identical in the presence and absence of the second substrate, **1** (Tables I and II). Again, this indicates that the formation of the complex of the substrate **2** and the protein is not significantly influenced by the second substrate, compound **1**.

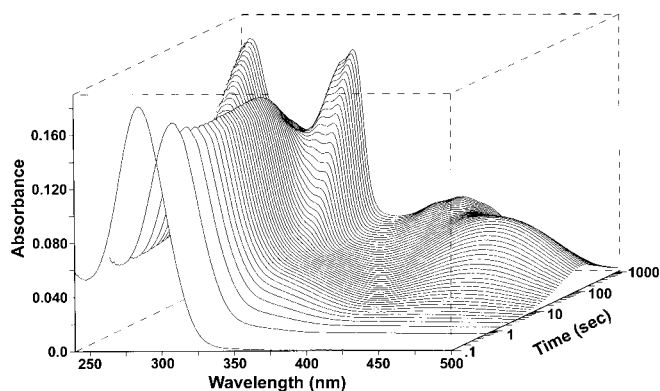


FIG. 6. **Presteady state kinetics of lumazine synthase.** A solution containing compound **1** and enzyme in 100 mM potassium phosphate, pH 6.9, was rapidly mixed with compound **2** in the same buffer at 25 °C. The concentrations after rapid mixing were 96 μM compound **2**, 500 μM compound **1**, and 105 μM lumazine synthase subunits. The dead time after mixing was 7.6 ms. Absorption spectra were recorded at intervals of 100 ms.

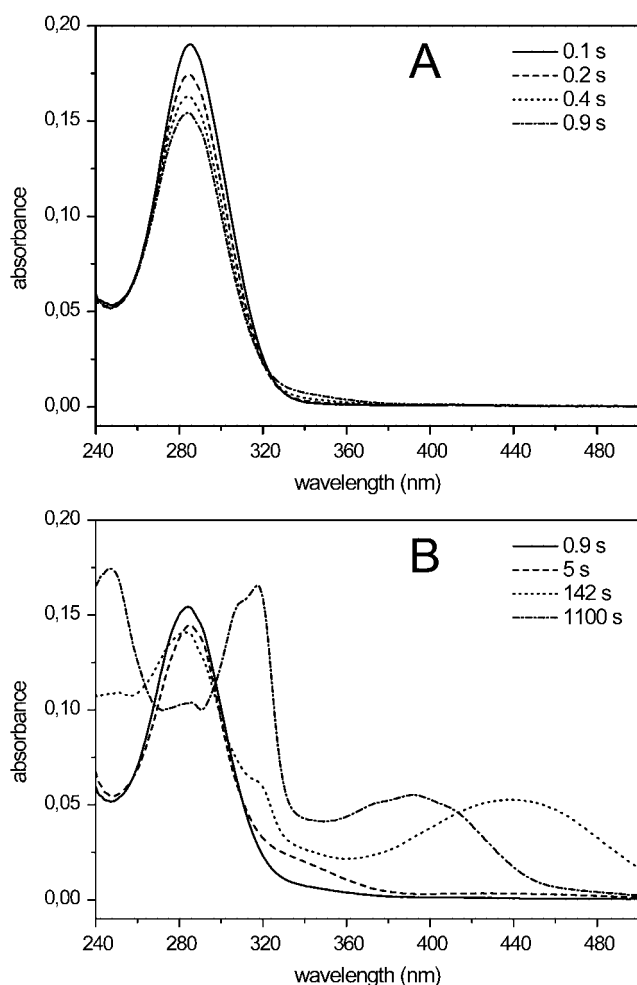


FIG. 7. **Ultraviolet spectra from the early (A) and the later phase (B) of the single turnover experiment shown in Fig. 6.** For details, see the legend for Fig. 6.

Our earlier experiments with the *B. subtilis* enzyme (17) had suggested the formation of a transient species with an absorption band around 320 nm, which was tentatively interpreted as the Schiff base **5** (compare Fig. 9). However, the transient species was so poorly populated that the spectrum could not be resolved by numerical deconvolution. In case of the *A. aeolicus* enzyme, this transient is more highly populated, and the spec-

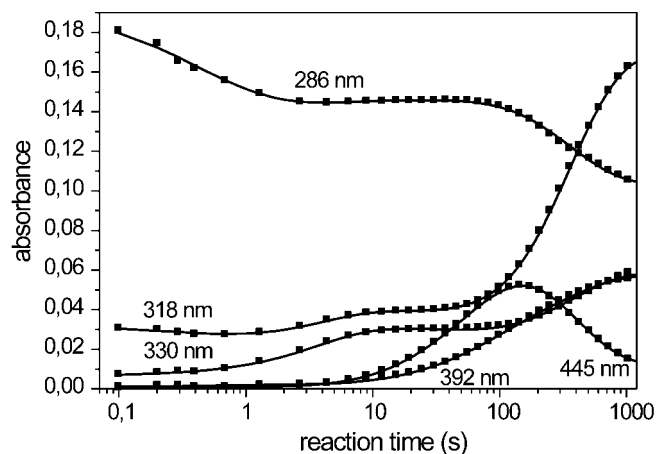


FIG. 8. **Absorbance changes obtained from single turnover experiment with lumazine synthase from *A. aeolicus*.** Symbols represent the original data, lines represent the data obtained from numerical simulation using the kinetic constants in Table I.

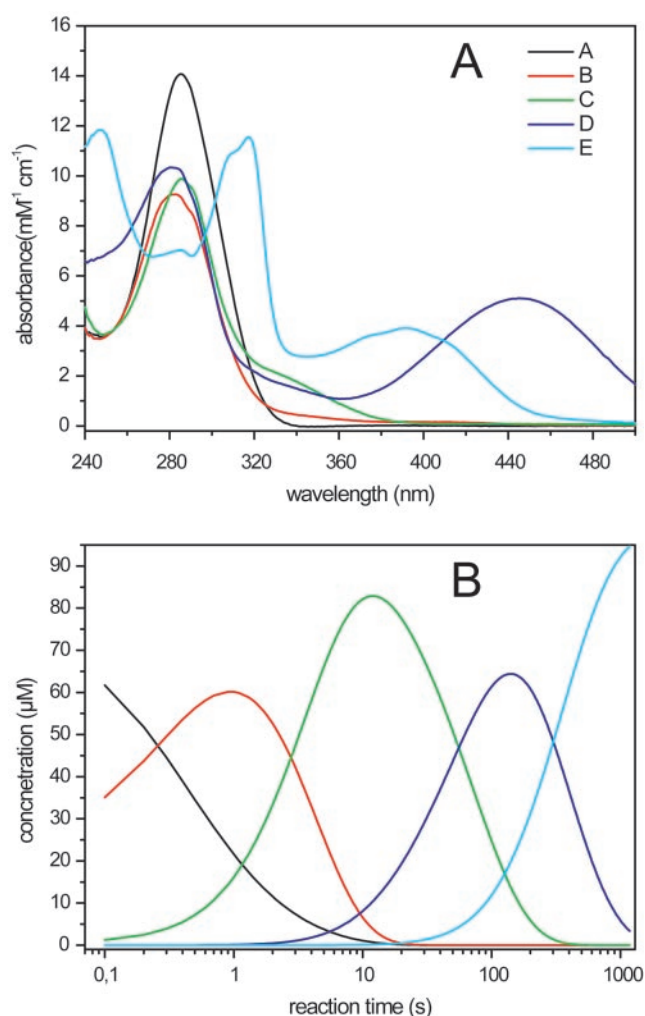


FIG. 9. **Numerical deconvolution of the stopped flow experiment shown in Fig. 6.** A, reconstructed absorbance spectra of transient chromophors. B, concentrations of transient species.

trum of the intermediate can be extracted numerically. It is characterized by a maximum at 330 nm, which is well in line with the expected properties of the hypothetical Schiff base intermediate **5**.

The subsequent intense transient with maxima at 282 and 445 nm has been described in our earlier study (17) and could

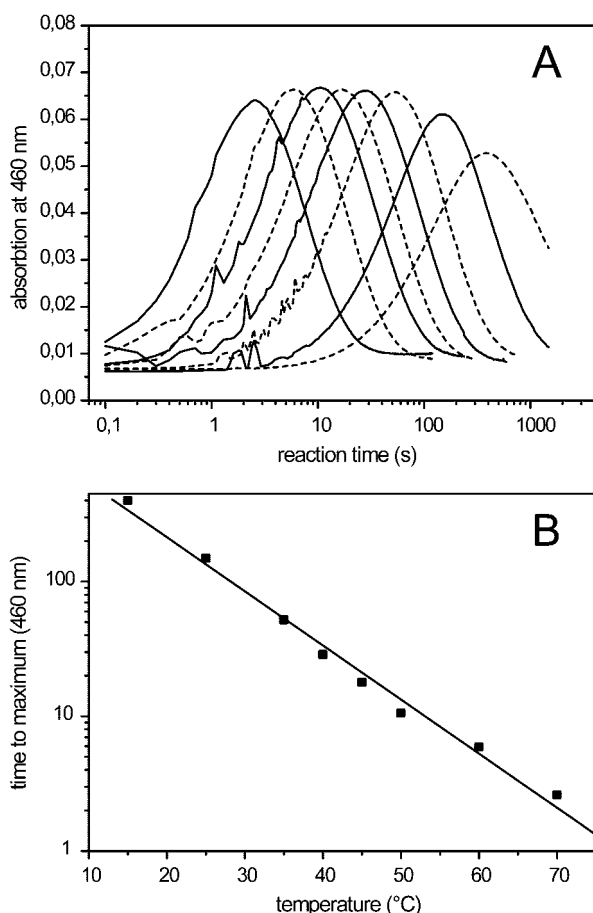


FIG. 10. A, time-dependent optical absorbance at 460 nm measured in stopped flow experiments. Temperatures are (from left to right): 70, 60, 50, 45, 40, 35, 25, and 15 °C. For experimental details, see the legend for Fig. 6. B, effect of temperature on the time to reach the maximum absorbance at 460 nm.

represent one of the intermediates **6** to **8**. The final stage of the reaction is characterized by maxima at 247, 317, and 391 nm and is virtually identical with the difference spectrum of **3** in complex with lumazine synthase. These spectra are substantially different from that of **3** in either neutral or alkaline solution. However, they are similar to the spectrum of 6,7,8-trimethylumazine **13** (Fig. 3) under alkaline conditions (Fig. 4B).

Under alkaline conditions, lumazine derivatives with position 8 side chains carrying hydroxy groups in the 2' or 3' position form tricyclic anions (Fig. 3, compounds **11** and **12**) through the addition of one of the side chain hydroxy groups to C-7 of the pteridine ring system (25, 26). The formation of such a tricyclic system is not possible for 6,7,8-trimethylumazine **13**, which forms an exomethylene structure instead (Fig. 3, compound **14**). An exomethylene type anion species **10** (Fig. 3) has also been shown by NMR spectroscopy to be present, albeit in very low amounts, in the equilibrium mixture of anionic species formed by 6,7-dimethyl-8-ribityllumazine under alkaline conditions (26, 27). The optical spectrum of **3** in alkaline solution is dominated by contributions of tricyclic species absorbing at 282, 313, and 366 nm (26); these spectral features are characteristic of the various species **10**, **11**, **12**. Closer inspection, however, reveals a weak band in the region above 340 nm, which is likely to represent the small amount of exomethylene anion **10** in the mixture. Based on these data, it appears that (i) the pK of **3** is decreased considerably upon binding the enzyme and that (ii) the fixation of the extended

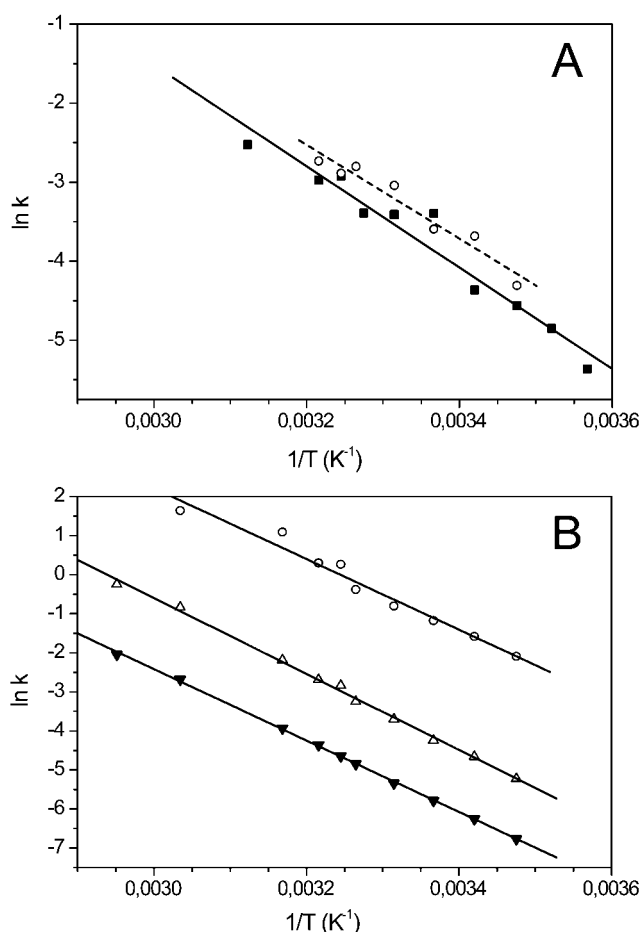


FIG. 11. A, Arrhenius plot for binding of compound **2** to lumazine synthase. ■, rate constant in the absence of compound **1** (for details, see the legend for Fig. 5); ○, k_1 from single turnover experiments using the mixture of both substrates (for details, see the legend for Fig. 6). B, Arrhenius plots for partial reactions catalyzed by lumazine synthase. ○, k_2 ; △, k_3 ; ▼, k_4 . For experimental conditions, see the legend for Fig. 6. Experiments were performed at temperatures ranging from 15 to 70 °C.

TABLE II
Activation parameters for binding of compound **2** to lumazine synthase from *A. aeolicus*

E_a	ΔG^\ddagger	ΔH^\ddagger	$-T\Delta S^\ddagger$	k (25 °C)
kJ mol^{-1}	kJ mol^{-1}	kJ mol^{-1}	kJ mol^{-1}	$\mu\text{M}^{-1} \text{s}^{-1}$
53.4 ± 4.3	82.4 ± 8.6	50.8 ± 4.3	31.6 ± 4.3	0.0224 ± 0.0051

ribityl side chain conformation precludes the formation of a tricyclic molecule. Thus, the exomethylene anion **10** is the dominant enzyme-bound species.

Due to the remarkable thermostability of the enzyme under study, stopped flow experiments could be performed in a wide temperature range from 15 to 70 °C. Naturally, the time frame of these experiments varies over a wide range. The spectra from all experiments could be deconvoluted numerically. To the best of our knowledge, this is the first study of enzyme pre-steady state kinetics over a wide range of temperatures.

The temperature dependence of the rate constants k_1 to k_4 is summarized in Fig. 11. They all obey a linear Arrhenius relation, and the slopes of the regression lines are all similar. This result provides evidence that there are no temperature-dependent conformational changes of the enzyme (28). Furthermore, the rate-determining step does not change within the temperature range measured (29). Thus, it comes as no surprise that the optical spectra obtained in stopped flow experiments develop in a closely similar manner over the entire temperature range studied.

Based on these data, an attempt has been made to extract the activation parameters for all rate constants from the kinetic data (Tables I and II). The activation energies for all steps in the complex reaction trajectory of lumazine synthase are remarkably similar. There are no thermodynamic holes for any of the intermediates to fall into. It should be mentioned that the activation parameters for the rate-determining step, *i.e.* the formation of **3** from the transient species D, are closely similar to the activation parameters obtained for the overall reaction by steady state kinetic analysis.

Acknowledgment—We thank Angelika Werner for expert help with the preparation of the manuscript.

REFERENCES

1. Neuberger, G., and Bacher, A. (1986) *Biochem. Biophys. Res. Commun.* **139**, 1111–1116
2. Kis, K., Volk, R., and Bacher, A. (1995) *Biochemistry* **34**, 2883–2892
3. Kis, K., and Bacher, A. (1995) *J. Biol. Chem.* **270**, 16788–16795
4. Volk, R., and Bacher, A. (1990) *J. Biol. Chem.* **265**, 19479–19485
5. Zhang, X., Meining, W., Fischer, M., Bacher, A., and Ladenstein, R. (2001) *J. Mol. Biol.* **306**, 1099–1114
6. Ritsert, K., Huber, R., Turk, D., Ladenstein, R., Schmidt-Bäse, K., and Bacher, A. (1995) *J. Mol. Biol.* **253**, 151–167
7. Ladenstein, R., Schneider, M., Huber, R., Bartunik, H. D., Wilson, K., Schott, K., and Bacher, A. (1988) *J. Mol. Biol.* **203**, 1045–1070
8. Mörtl, S., Fischer, M., Richter, G., Tack, J., Weinkauff, S., and Bacher, A. (1996) *J. Biol. Chem.* **271**, 33201–33207
9. Persson, K., Schneider, G., Jordan, D. B., Viitanen, P. V., and Sandalova, T. (1999) *Protein Sci.* **8**, 2355–2365
10. Ladenstein, R., Ludwig, H. C., and Bacher, A. (1983) *J. Biol. Chem.* **258**, 11981–11983
11. Bacher, A., Baur, R., Eggers, U., Harders, H. D., Otto, M. K., and Schnepfle, H. (1980) *J. Biol. Chem.* **255**, 632–637
12. Bacher, A., Schnepfle, H., Mailänder, B., Otto, M. K., and Ben-Shaul, Y. (1980) in *Proceedings of the 6th International Symposium on Flavins and Flavoproteins*, pp. 579–586, Japanese Science Society Press, Tokyo, Japan
13. Bacher, A., Ludwig, H. C., Schnepfle, H., and Ben Shaul, Y. (1986) *J. Mol. Biol.* **187**, 75–86
14. Bacher, A., and Ladenstein, R. (1991) in *Chemistry and Biochemistry of Flavoenzymes* (Müller, F., ed) Vol. 1, pp. 293–316, CRC Press, Inc., Boca Raton, FL
15. Meining, W., Mörtl, S., Fischer, M., Cushman, M., Bacher, A., and Ladenstein, R. (2000) *J. Mol. Biol.* **299**, 181–197
16. Zhang, X., Meining, W., Cushman, M., Haase, I., Fischer, M., Bacher, A., and Ladenstein, R. (2003) *J. Mol. Biol.* **328**, 167–182
17. Schramek, N., Haase, I., Fischer, M., and Bacher, A. (2003) *J. Am. Chem. Soc.* **125**, 4460–4466
18. Zheng, Y.-J., Viitanen, P. V., and Jordan, D. B. (2000) *Bioorg. Med. Chem.* **28**, 89–97
19. Richter, G., Krieger, C., Volk, R., Kis, K., Ritz, H., Götze, E., and Bacher, A. (1997) *Methods Enzymol.* **280**, 374–382
20. Cresswell, R. M., and Wood, H. C. S. (1960) *J. Chem. Soc.* 4768–4775
21. Bacher, A. (1986) *Methods Enzymol.* **122**, 192–199
22. Fischer, M., Haase, I., Kis, K., Meining, W., Ladenstein, R., Cushman, M., Schramek, N., Huber, R., and Bacher, A. (2003) *J. Mol. Biol.* **326**, 783–793
23. Fischer, M., Haase, I., Feicht, R., Richter, G., Gerhardt, S., Changeux, J.-P., Huber, R., and Bacher, A. (2002) *Eur. J. Biochem.* **269**, 519–526
24. Haase, I., Mörtl, S., Kohler, P., Bacher, A., and Fischer, M. (2003) *Eur. J. Biochem.* **270**, 1025–1032
25. Pfeleiderer, W., Bunting, J. W., Perrin, D. D., and Nübel, G. (1966) *Chem. Ber.* **99**, 3503–3523
26. Beach, R. L., and Plaut, G. W. E. (1971) *J. Org. Chem.* **36**, 3937–3943
27. Bown, D. H., Keller, P. J., Floss, H. G., Sedlmaier, H., and Bacher, A. (1986) *J. Org. Chem.* **51**, 2461–2467
28. Massey, V., Curti, B., and Ganther, H. (1966) *J. Biol. Chem.* **241**, 2347–2357
29. Kistiakowsky, G. B., and Lumry, R. (1949) *J. Am. Chem. Soc.* **71**, 2006–2013